Pulsatory andesite lava flow at Bagana Volcano

Geochemistry Geophysics Geosystems G3

Article
Volume 13, Number 11
27 November 2012
Q11011, doi:10.1029/2012GC004336
ISSN: 1525-2027

Published by AGU and the Geochemical Society

Pulsatory andesite lava flow at Bagana Volcano

G. Wadge
National Centre for Earth Observation, ESSC, University of Reading, Reading RG6 6AL, UK (g.wadge@reading.ac.uk)

S. Saunders and I. Itikarai
Rabaul Volcano Observatory, Rabaul, Papua New Guinea

[1] Using a time series of TerraSAR-X spaceborne radar images we have measured the pulsatory motion of an andesite lava flow over a 14-month period at Bagana Volcano, Papua New Guinea. Between October 2010 and December 2011, lava flowed continuously down the western flank of the volcano forming a 3 km-long blocky lava flow with a channel, levees, overflows and branches. We captured four successive pulses of lava advancing down the channel system, the first such behavior of an andesite flow to be recorded using radar. Each pulse had a volume of the order of 10^7 m^3 emplaced over many weeks. The average extrusion rate estimated from the radar data was 0.92 ± 0.35 m^3 s^{-1}, and varied between 0.3 and 1.8 m^3 s^{-1}, with higher rates occurring earlier in each pulse. This, together with observations of sulphur dioxide emissions, explosions and incandescence suggest a variable supply rate of magma through Bagana's conduit as the most likely source of the pulsatory behavior.

Components: 7400 words, 9 figures, 3 tables.

Keywords: Bagana; andesite lava flow; pulsatory flow.

Index Terms: 8414 Volcanology: Eruption mechanisms and flow emplacement; 8429 Volcanology: Lava rheology and morphology; 8485 Volcanology: Remote sensing of volcanoes (4337).

Received 11 July 2012; **Revised** 11 October 2012; **Accepted** 15 October 2012; **Published** 27 November 2012.

Wadge, G., S. Saunders, and I. Itikarai (2012), Pulsatory andesite lava flow at Bagana Volcano, *Geochem. Geophys. Geosyst.*, *13*, Q11011, doi:10.1029/2012GC004336.

1. Introduction

[2] Lava flows are gravity currents of viscous or viscoplastic liquid whose advance is controlled by the rate of extrusion at the source vent, the rheology of the bulk flow and the surface environment over which they move [*Griffiths*, 2000]. The morphology of the final, frozen flow can be the result of a complex history of time- and space-varying factors during its emplacement, for example, the formation of channels, levees, tubes and branching flow. The large surface area and hazardous conditions on some lava flows make it difficult to monitor how the flows develop. As a result, infrequent observations can miss or alias flow dynamics. In this context, the advance of silicic lava flows, which tend to be thicker and slower than more mafic flows, reduces the need for very frequent observations to capture the character of their flow. However, silicic lava flows are less common than their more mafic counterparts and often less amenable to field access. As a result there are only a few studies of the dynamics of andesite and dacite lava flow emplacement at, for example, Arenal [*Borgia et al.*,

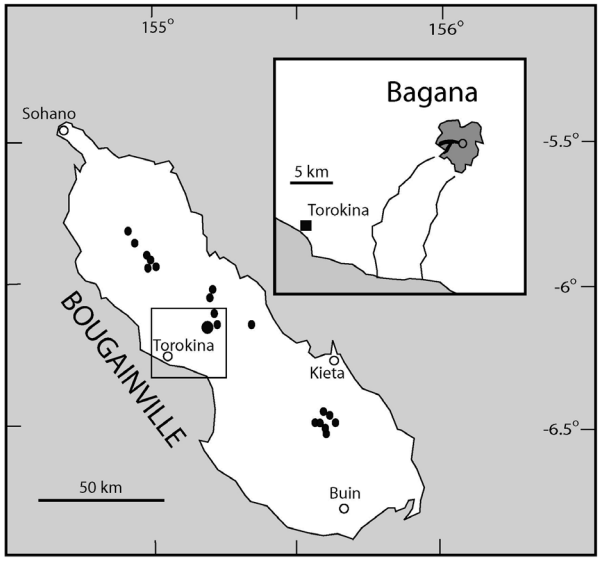

Figure 1. Outline map of Bougainville island, Papua New Guinea. The Solomon Sea subduction zone is to the southwest. The main towns are labeled and the black circles are Cenozoic volcanic centers forming the volcanic front. The rectangle shows the location of Bagana Volcano. The inset expands this area to sketch the outline of the Bagana lava flow field (dark gray), the 2010–2011 flow to the west of the summit crater (black), and the two main rivers that drain the volcanic sediments to the southwest.

1983; *Cigolini et al.*, 1984], at Lonquimay [*Naranjo et al.*, 1992] and at Santiaguito [*Harris et al.*, 2003, 2004].

[3] In this paper we present a 14-month (October 2010–December 2011) observational record of the emplacement of an andesite lava flow on the western slopes of Bagana Volcano, Papua New Guinea (PNG). Ground-based observations of the volcano during this period were limited to a daily report by a single observer, who could not see the flow. The main observations reported here were made from space using the TerraSAR-X (TSX) radar, at a frequency of up to every 11 days. These data allowed us to measure the dimensions of the flow and its rate of advance and from these to estimate the lava extrusion rate. We observed four distinct pulses of lava over the 14-month period. Although ad hoc observations of pulsatory lava flow have been made in the field before, this is the first set of synoptic radar measurements of pulsating silicic lava flows. After a brief introduction to Bagana Volcano, we describe how we used the radar data to measure the advance and emplacement of the lava in these pulses. We also relate these measurements to other ground-based observations of explosive activity and satellite observations of gas emission, followed by a discussion of the dynamics and physical mechanisms that might be responsible for the pulses.

2. Bagana Volcano

[4] Bagana Volcano (06°09′S; 155°11′E) sits on Bougainville island where the Solomon Sea Plate subducts beneath the Pacific Plate (Figure 1). Bagana has produced a succession of andesitic lava flows from a central vent since the 1870s at least [*Bultitude*, 1976]. The typical pattern of activity is for near-continuous extrusion of lava within a shallow, dome-filled summit crater that spills out onto steep (∼40°) slopes on which a strongly channelized flow develops. Blocky flows extend up to 3–4 km, and compound flow fields may take several years to be emplaced [*Bultitude*, 1976, 1981]. Relatively modest Vulcanian explosions with tephra dispersal occur every few weeks to months. Every few years there are larger explosions producing tephra clouds and pyroclastic density currents. To the southwest of the volcano is an apron of volcaniclastic sediments that drains to the sea (Figure 1). Bagana has a continuous plume of gas, with the SO_2 flux measured from the ground in 2003 as $\sim 725 \times 10^6$ kg/yr [*McGonigle et al.*, 2004] and from space between 2005 and 2008 as $\sim 114 \times 10^6$ kg/yr [*McCormick et al.*, 2012], the strongest SO_2 flux of any Papua New Guinea volcano. In recent years the population close to the volcano, particularly to the southwest, has increased. There is the need for improved monitoring, including the use of remotely sensed data, to help assess the hazards posed.

[5] The surface of the lava flows are covered by blocks of angular, smooth-sided, massive to vesicular, andesite up to several meters across [*Bultitude*, 1976, 1981]. The flows are thick (tens of meters), about 100 m wide on the steep upper slopes, broadening to about 200–300 m wide on the lower slopes. Well-defined channels between 60 and 150 m wide form in the middle section of the flow. The flows sometime branch, as occurred in the case described here, to produce a compound, lobate field with transverse ridges. Talus and minor ash accumulate between flows. As the lava flows age they are increasingly colonized by vegetation, particularly on the lower slopes.

[6] The Bagana andesites have 30–50% phenocrysts, mainly plagioclase, with minor clinopyroxene and iron-titanium oxides and sparse, large

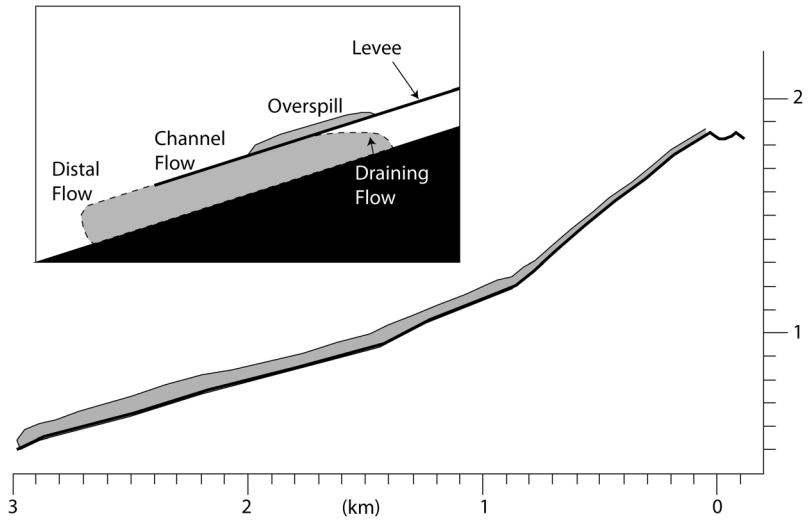

Figure 2. True-scale profile of the medial line course of the active lava flow on the west of Bagana in 2011 (elevation in m above sea level). The gray represents the flow. The inset panel shows a schematic down-flow section whose main volumetric elements comprising a pulse of lava moving through a channel are as follows: the distal flow regime that is unconstrained, channel flow in which the lava is constrained by earlier formed levees and may be drained behind, and any lava that overspills the levees to leave a separate lava deposit.

(up to 2.5 cm) brown hornblende phenocrysts [*Bultitude et al.*, 1978]. Microphenocrysts are mainly of orthopyroxene with rare olivine, and the groundmass is either glassy or a microcrystalline mix of plagioclase, clinopyroxene, oxides and apatite. There are rare enclaves of a dacitic composition. The whole-rock silica content of the lavas ranges from 53 to 58%, placing them on the basic side of the andesite range [*Gill*, 1981]. The high phenocryst content means that the lavas will have a touching network of crystals capable of producing a non-Newtonian rheology. We assume that the 2010–11 lavas are of similar composition to these earlier lavas.

3. Radar Observations

[7] We have used TSX, X-band (~3 cm), radar images collected from space to detect the motion of lava flows on Bagana Volcano between October 2010 and December 2011. The images were collected in "spotlight mode" at ~2.5 m per pixel sampling size from descending passes of the satellite, with the radar looking to the west along an azimuth of 282°, at an angle to the vertical of 23.8°. The gross topographic distortion of the radar images has been corrected by use of a DEM created from Shuttle Radar Topography Mission (SRTM) data and mapped in the UTM projection (the EEC product). However, the post-2000 lava flows have not been corrected in this way and do show local distortion. *Breit et al.* [2010] gives full details of TSX data products.

[8] We used the intensity of these images to extract two types of information: flow motion derived from pairs of images with the same viewing geometry used in change difference configuration, and the radar shadowing created by the steep inner walls of the flow channels and the distal levees were used to estimate the depth of lava. We discovered that there was only one active lava flow during this interval, flowing from the summit crater to the west southwest. This flow reached a maximum distance of about 3 km in two branches. For the first 800 m below the crater the gradient was about 39° (the angle of repose of blocky lava), and the gradient of the furthest 1.5 km of flow was about 15° (Figure 2). There were also changes in the radar images suggesting rockfall-derived talus deposition to either side of the proximal lava levees and from the crater, but these are mostly minor. Table 1 shows the dates of the images used.

[9] The value of change difference TSX images for detecting and quantifying volcanic activity was demonstrated by *Wadge et al.* [2011] for pyroclastic density current deposits on Soufrière Hills Volcano, Montserrat. We used their display procedure: the earlier image is assigned to the red channel, the later image to the green channel and the scaled difference image to the blue channel of an r:g:b display. Those parts of the display with increased reflectivity in the later image (green

Table 1. TSX-measured Flow Advance for Each of the Four Pulses of Lava

Image Dates	Int. (days)	P0 len (incr)	P1 len (incr)	P2 len (incr) [over:chan]	P3 len (incr) [over:chan]
25Oct10–5Nov 2010	11	2950 (20)	700 (700)		
5Nov–30Dec 2010	55	3000 (50)	1400 (700)		
30Dec–21Jan 2011	22	static	1500 (100) [:1000]		
21Jan–6 Mar 2011	44		1600 (100) [:1100]	900 (900) [700:1000]	
6Mar–17 Mar 2011	11		static	1200 (300) [800:]	
17 Mar–28 Mar 2011	11			1400 (200) [1000:]	
28 Mar–8 Apr 2011	11			1550 (150) [1100:]	
8 Apr–19 Apr 2011	11			1700 (150) [1200:1100]	
19 Apr–11 May 2011	33			2000 (300) [1500:1300]	
11 May–22 May 2011	11			2200 (200) [1700:1500]	
22 May–13 Jun 2011	22			2500 (300) [2000:1500]	
13 Jun–24 Jun 2011	11			2600 (100)	
24 Jun–5 Jul 2011	11			2750 (150)	
5 Jul–16 Jul 2011	11			2800 (50)	
16 Jul–27 Jul 2011	11			2850 (50)	
27 Jul–7 Aug 2011	11			2900 (50)	
7 Aug–9 Sep 2011	33			3000 (100)	
9 Sep–23 Oct 2011	44			static	1300 (1300)
23 Oct–6 Dec 2011	44				1500 (200) [1100:]

[a]Int =time interval. Len = length of flow (m). Incr = incremental increase in flow length (m). Over= distance along flow to back of overflow of lava onto levees (m). Chan= distance along flow to end of the drained lava channel (m).

channel) have a cyan color, those with decreased reflectivity in the later image have a magenta color. Those parts of the scene that are unchanged are displayed as yellow.

[10] Figure 3 shows a typical change difference image of the active lava flow representing change between 5 November and 30 December 2010. The general morphology of the flow can be appreciated from the intensity shading, with various areas of cyan and magenta superimposed. At the front of the flow is a dual band of magenta and cyan that corresponds to the distal zone in which the lava spreads laterally to form levees [*Hulme*, 1974]. The magenta represents the talus slope forming ahead of the lava flow proper [c.f. *Borgia et al.*, 1983], which because of its orientation reduces the backscattering intensity of the later image. The cyan-colored band represents the flatter, extending, surface of the lava itself, as it rolls over beneath the talus (Figure 3a). The radar illumination is such that those parts of the flow with a deep central channel have a bright (yellow) inner channel wall on the northern side, and a shadowed (black) inner channel wall on the southern side (Figure 3b). Higher up the flow, new lava has filled the channel reducing the bright reflections from the channel's northern inner wall, seen as a strip of magenta, while the formerly shadowed southern side of the channel also returns reflections from the new lava but this now has a higher reflectivity and is seen as a strip of cyan (Figure 3c). Elsewhere, over most of the flow there are areas of cyan and magenta that are less easily interpreted in terms of local morphology but clearly represent change in the intensity of backscatter of the radar which we interpret as local change in the surface slope or "roughness" of the lava at the meter scale, caused by flow motion. Figures 4 and 7 also show other examples of the change difference images. Subtle differences in the reflectivity of the stationary lava flow surfaces can be seen in these images. These differences are probably due to the vegetation-related changes mentioned earlier. For example, in Figure 4 it can be seen that the flow underlying the 2010–2011 flow has a similar hue and reflectivity to that of Pulse 0 by the time of Figure 4d, but is distinct from the flow below it.

4. Other Observations

4.1. Ground-Based

[11] The activity of Bagana was reported daily (except in mid-October 2011) by an observer situated about 16 km to the southwest. The state of the gas plume, the occurrence of any atmospheric glow due to lava incandescence, and any auditory phenomena were recorded in addition to general meteorological conditions. Although basic, and subject to obscuration by clouds, these observations proved useful (Figure 5), though major variations in the vigor of the gas plume could not be detected

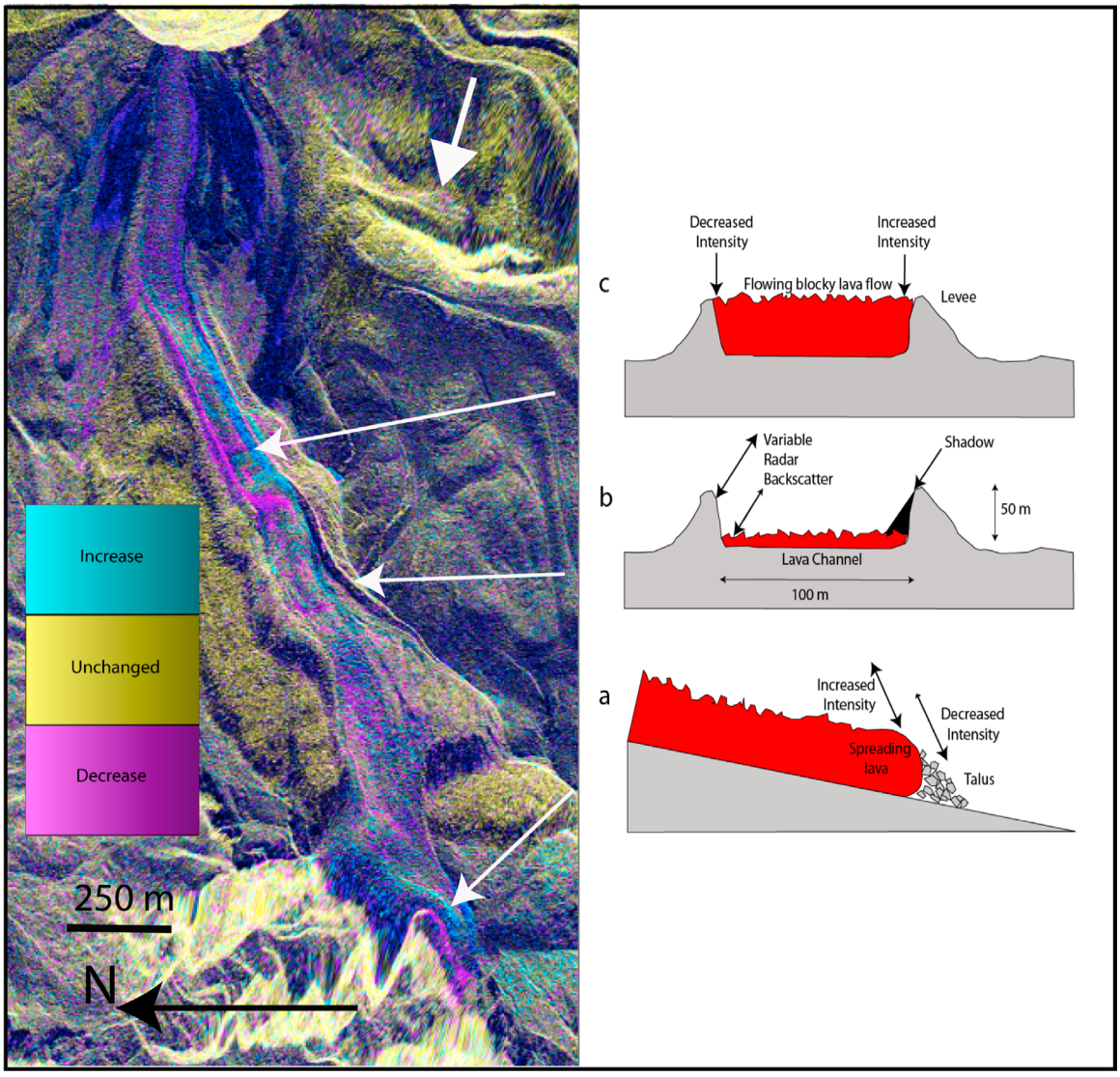

Figure 3. TSX change difference image of the active lava flow on the west flank of Bagana between 5 November and 30 December 2010. Radar illumination direction is shown by the thick white arrow. The cyan and magenta hues represent increased and decreased radar backscatter intensity over the period respectively. (a) A schematic along-flow section showing the reduced intensity (magenta) of the flow front talus and increased intensity (cyan) of the spreading lava. (b) A schematic across-flow section showing the typical shadowed and illuminated walls of a drained channel. (c) A schematic across-flow section showing how a newly filled channel has distinctive magenta and cyan stripes in the positions of the channel walls.

readily from the ground. Incandescent glow could be detected from the central crater/lava dome and also from the western rim where the active lava flow spilled out. Two types of auditory signal were evident: a distinct, single or multiple explosion ("boom") and a semi-continuous to continuous "jet-engine type roar." The explosions were often accompanied by modest tephra clouds rising up to 500 m above the lava dome. The roaring noise continued in some instances for over one day, but was not linked to visible ash clouds.

4.2. SO_2 Loading From Satellite

[12] We have tracked the sulphur dioxide loading of the atmosphere produced from Bagana using the daily measurements by the OMI sensor on-board the Aura satellite [e.g., *McCormick et al.*, 2012]. There are gaps in the coverage but the data set does appear to reflect major changes in the vigor of sulphur dioxide output by the volcano. We have used the OMI data [so2.gsfc.nasa.gov] qualitatively for this study; classifying the daily atmospheric

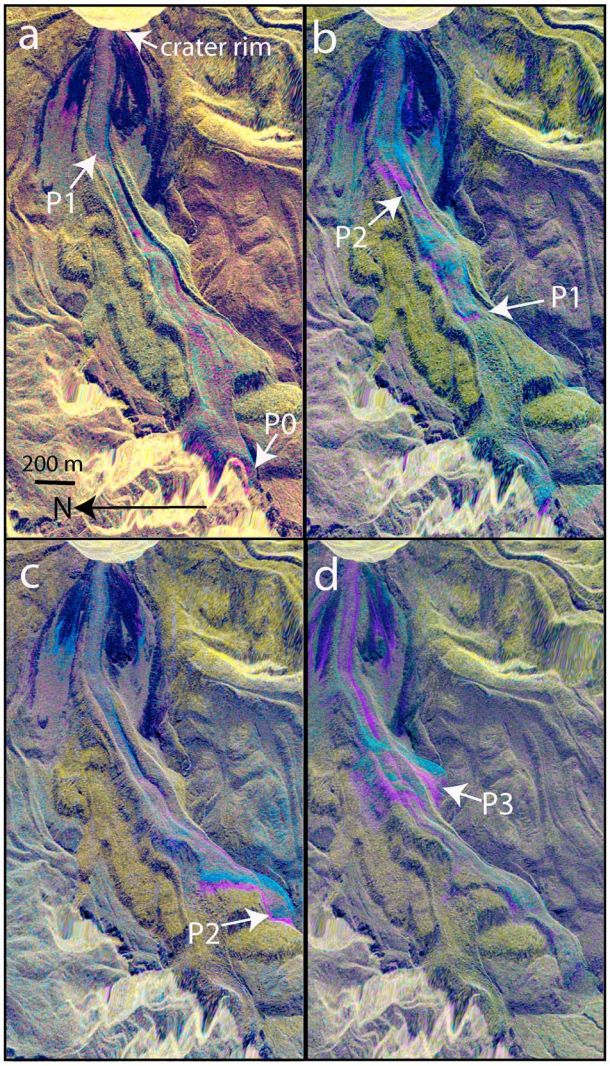

Figure 4. Selected examples of change difference images. (a) 25 October–5 November 2010: the advancing front of P1 is shown, as is the, almost stationary, front of P0. (b) 21 January–6 March 2011: P1 is still moving, very slowly, while the front of P2 advances much faster with some overflow. (c) 22 May–13 June 2011: P2 has branched from the P0 channel and is spreading rapidly down another valley. (d) 23 October–6 December 2011 (note this image is offset to the south): P2 is now static and P3 has advanced about 1.5 km and overflowed its levees.

loading due to Bagana on a five-point scale: nil, weak, moderate, strong and very strong (Figure 5).

4.3. Thermal Emissions From Satellite

[13] We have studied the available MODIS and ASTER thermal and short-wave infrared satellite images of Bagana for several years leading up to 2011. There is no evidence of major breaks in effusive activity since 2000. The 90 m-resolution ASTER data show that there was a change in direction of lava flow, from southwest to west, out of the summit crater in 2008. However, cloud cover is too great generally at Bagana to be able detect the temporal variability of thermal emission at the time scale of the pulses as in Figure 5.

5. Measuring the Changing Lava Flow

5.1. Advance of the Flow

[14] The first change difference image in the sequence (25 October–5 November 2010) (Table 1 and Figure 4a) showed the flow with a heavily shadowed, drained channel. Downstream, the distal surface showed subtle changes indicating slow advance of the lava flow, termed P0, which was probably several months old by this time. In the steep, proximal part of the flow, a new pulse of lava (P1) had advanced up to 700 m during the 11-day interval. There was then a gap in the data of 55-days during which P1 advanced through the steep-walled channel by another 700 m (Figure 3). However, the distal front of P0 also advanced by several tens of meters in the same period. During the next interval (30 December 2010–21 January 2011) P0 is seen to have stopped advancing, while P1 flows another ~100 m in the channel. By 6 March 2011 another new pulse of lava (P2) had advanced 900 m down the upper channel, with a steep front (Figure 4b), while P1 had advanced only a few tens of meters. Between 6 March and 19 April 2011, four 11-day change difference images show that P2 slowed and overflowed the levees on either side of the channel. As it reached the now static front of P1 around 19 April 2011, P2 left the P0/P1 channel entirely and started to flow down a valley to the southwest. Upstream, the depth of lava in the channel then fell as the distal flow of the new pulse accelerated during May 2011 (Figure 4c). By the end of June 2011 the rate of flow advance had slowed, but continued until the P2 flow reached a maximum length of 3 km around early September 2011. By the time of the next image, 23 October 2011, a new pulse of lava (P3) had advanced about 1.3 km within the upper channel (Figure 5), though P2 showed contemporary evidence of minor motion. P3 advanced another ~200 m by 6 December 2011 but had also spilled over the levees near the same location as occurred for the P2 pulse in March–April 2011, with a new incipient flow to the south (Figure 4d). P3 probably came to a halt soon after, in late December 2011. After this an entirely new flow developed.

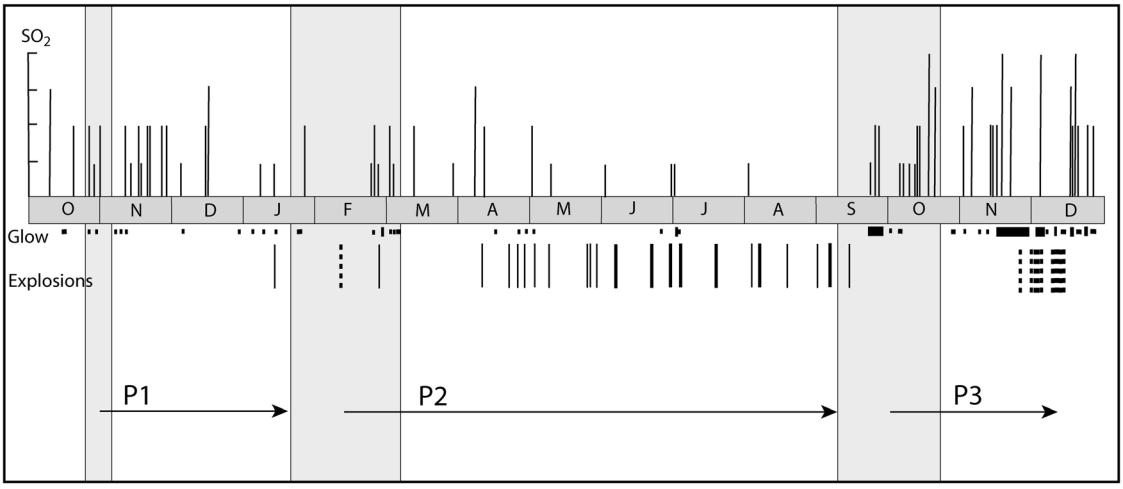

Figure 5. Daily timeline (letters in dark gray bar denote months of 2010 and 2011) of ground and satellite observations. Above the bar the vertical black lines represent the atmospheric loading of sulphur dioxide measured by OMI on a qualitative 5-class scale. Immediately below the bar are the observations of crater glow as black blocks (the taller blocks denoting brighter glow). Below that are vertical black lines representing explosions (the thicker lines represent accompanying tephra) and dashed vertical lines representing jet-like venting. The three vertical gray bars show the uncertainty in the timing of the onset of pulses P1–P3.

[15] The evolution of the four pulses (P0–P3) measured over 14 months is shown schematically in Figure 6 and the flow advance distances given in Table 1. The width of the channel was measured at 100 m intervals along the flow for each image pair. Although the pixel size of the data is 2.25 m, we measured the length and width of the flow to the nearest 10 m and estimated the uncertainty on that as $\pm$10 m. In Figure 4 the incremental advance of the front of P2 is mapped in the medial and distal parts. P0 and P2 both attained lengths of about 3 km (Figure 5) and used a common channel as far as 1.6 km from the crater, but branched beyond that point, with the P0 flow emplaced to the west and the P2 flow to the southwest. The pulsatory nature of the flow can be best appreciated in the animation of the TSX change difference images between October 2010 and August 2011 (see auxiliary material).[1] The onsets of pulses P1–3 are loosely constrained by the TSX data to: no later than 25 October–5 November 2010 (P1), 21 January–6 March 2011 (P2) and 9 September–23 October 2011 (P3).

5.2. Flow Thickness, Volume and Extrusion Rate

[16] For any given interval there may have been changes in five components of the volumetric budget of lava extrusion:

[17] i) distal flow spreading ahead of the channel over unconstrained terrain,

[18] ii) lateral overflow out of the channel onto the levees,

[19] iii) flow of lava within or drainage down the channel,

[20] iv) changing shape of the summit lava dome,

[21] v) rockfall-talus flanking the proximal lava channel.

[22] We cannot distinguish between (iii) and any in situ inflation/deflation of the lava surface. TSX gives very little information about the lava dome and here we assume it had a steady state shape. Occasionally the talus around the crater changed its TSX signature, but the volumes involved cannot be gauged and we ignore them here. We concentrate on estimating (i)-(iii), shown schematically in Figure 2.

[23] The most up-to-date topography of Bagana is the SRTM DEM acquired in 2000 and used in the radar terrain correction. However, we have no such DEM with an absolute datum to calculate the elevation of the 2010–11 lava flow. Hence our volumetric estimates are based on the areas of flow advance, the heights of the flows from shadowing, the slope of levees and, in the most distal parts of the flow advancing over new terrain, the SRTM DEM.

[1]Auxiliary materials are available in the HTML. doi:10.1029/2012GC004336.

Table 2. Incremental Volume Components and Extrusion Rates

Pulse	Interval	Chan. Volume (10^3 m^3)	Distal Volume (10^3 m^3)	Overfl. Volume (10^3 m^3)	Total Volume (10^3 m^3)	Cumul. Volume (10^3 m^3)	Extrusion Rate (m^3 s^{-1})
P0	25Oct–5Nov 2010						
P0	5Nov–30Dec 2010		2300		2300 (±506)	2300	0.48 (±0.11)
P1	25Oct–5Nov 2010	1680	-	-	1680 (±470)	3980	1.8 (±0.5)
P1	5Nov–30Dec 2010	3281	-	-	3281 (±919)	7261	0.69 (±0.19)
P1	30Dec–21Jan 2011	494	-	-	494 (±138)	7755	0.26 (±0.07
P2	21Jan–6Mar 2011	2350	-	350	2700 (±969)	10455	0.71 (±0.25)
P2	6 Mar–17 Mar 2011	504	-	250	754 (±363)	11209	0.79 (±0.38)
P2	17Mar–28Mar 2011	462	-	600	1062 (±663)	12271	1.1 (±0.69)
P2	28Mar–8Apr 2011	845	-	350	1195 (±548)	13466	1.3 (±0.6)
P2	8Apr–19Apr 2011	448	-	450	898 (±525)	14364	0.94 (±0.55)
P2	19Apr–11May 2011	−1333	4031	600	3298 (±1794)	17662	1.2 (±0.65)
P2	11May–22May 2011	−496	1875	-	1379 (±551)	19041	1.4 (±0.56)
P2	22May–13June 2011	437	2790	-	3227 (±736)	22268	1.7 (±0.39)
P2	13June–24June 2011	-	852	-	852 (±187)	23120	0.9 (±0.2)
P2	24June–5July 2011	231	542	-	773 (±184)	23893	0.81 (±0.19)
P2	5July–16July 2011	-	542	-	542 (±119)	24435	0.57 (±0.13)
P2	16July–27July 2011	−328	680	-	352 (±242)	24787	0.37 (±0.25)
P2	27July–7Aug 2011	−225	595	-	370 (±194)	25157	0.39 (±0.2)
P2	7Aug–9Sept 2011	363	765	-	1128 (±270)	26285	0.40 (±0.1)
P3	9Sept–23Oct2011	2768	-	1000	3768 (±1165)	30053	1.0 (±0.31)
P3	23Oct–6Dec 2011	674	-	1900	2574 (±1880)	32627	0.68 (±0.5)

[24] Out to about 2 km from the crater there was a well-developed channel that repeatedly filled and drained during the observation period. We do not know the full thickness of the channelized flow, but it must be greater than the maximum observed change in flow surface within it, about 60 m. The first 600 m of flow on the steepest slope (Figure 2) was at too acute an angle to the radar look-direction to allow channel drainage to be measured there. As a pulse passed down the channel it filled it and entered into the distal zone of lateral spreading to form its own levees, which then became the channel walls (component i). Sometimes, as the supply of lava weakened, the lava drained downflow, revealing an increased depth of channel. This volume drained from the channel contributed to the distal volume (iii) (Figure 2). *Harris et al.* [2004] used solar shadowing to estimate lava levee heights at Santiaguito. Here we used radar shadowing [*LaPrade and Leonardo*, 1969; *Wadge et al.*, 2011] to estimate the depth of flow in the lava channel and also the height of the distal levees to the nearest 5 m with an estimated uncertainty of ±7 m. The angle of repose of the blocky talus that mantles the sides of andesite lava levees [*Borgia et al.*, 1983] and lava domes [*Wadge et al.*, 2008] falls in the range 38–42°, and we used 40° here to validate the shadowing estimates.

[25] Pulses 2 and 3 both showed episodes of lava overflow onto the levees between 700 and 2000 m from the crater from March to June 2011 for P2, and from October to December 2011 for P3 (Table 1). The thickness of these overflows can't be detected from TSX data, but we assume a thickness of 20 m with an uncertainty of ±15 m. For P1–2, the TSX images record the filling and draining of the channel for each pulse. For P3 we see only the filling (and overflow) stage.

[26] The total incremental volume added during each measurement interval comprises:

$$\text{Total volume} = \text{distal volume} + \text{channel (full} - \text{drained) volume} + \text{overflow volume.}$$

[27] These are calculated using the areas of the distal, channel and overflow components multiplied by the distal levee heights, channel depth changes and an assumed 20 m overflow thickness respectively (Table 2). The incremental volume change from one image pair to the next gives the time-averaged volumetric discharge rate [*Harris et al.*, 2007] for that interval. We use the term extrusion rate for this here.

[28] The total volume of lava erupted as lava flows at Bagana between 25 October 2010 and 6 December 2011 is estimated as 32.6 ± 12 × 10^6 m^3 (not dense-rock equivalent). Most of this was erupted in P2 (18.5 × 10^6 m^3), with smaller volumes associated with P1 (5.5 × 10^6 m^3) and P3 (6.3 × 10^6 m^3). The volume estimated for

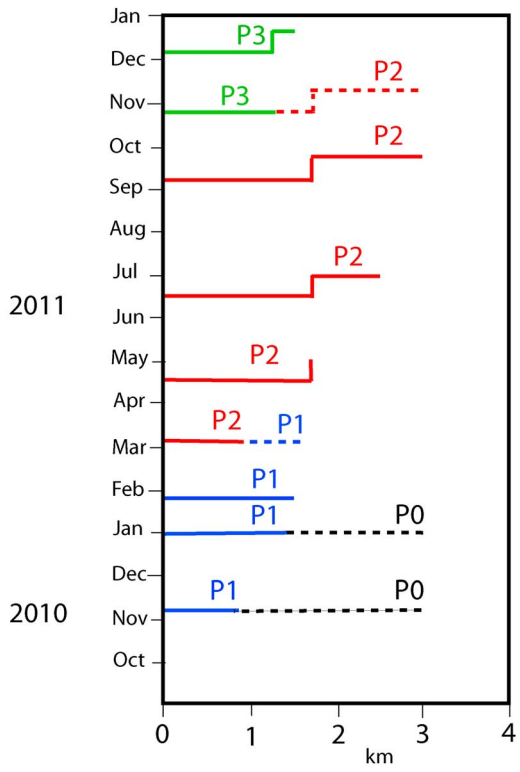

Figure 6. Schematic evolution of the four pulses of lava flow (P0–P3). Each horizontal line represents the length of the lava flow at the time of a radar image as ascertained by the change difference image for the preceding interval. The summit crater is at 0 km. Not all dates are shown for clarity. Solid lines are the dominant upstream pulses. Dashed lines are the older pulses that are still moving but much more slowly than the later pulse. The offsets to P2 and P3 begin at distances where the lava flow left the original main channel.

P0 (2.3×10^6 m^3) only represents the very end of this pulse, which also overlapped with pulse 1. The average extrusion rate for the whole period is 0.92 ± 0.35 m^3 s^{-1} and the rates by pulse as calculated according to the intervals in Table 2 are: P0 = 0.48 m^3 s^{-1}, P1 = 0.72 m^3 s^{-1}, P2 = 0.95 m^3 s^{-1}, P3 = 0.84 m^3 s^{-1}. Figure 6 shows the extrusion rate calculated by imaging interval. The rates were high at the start of P1 and P3 and fell toward the end. P2 only reached its maximum rate during the middle of the pulse. The dynamic bulk viscosity of the flow advance of P2 can be estimated from the Jeffery equation [c.f. *Harris et al.*, 2004] as about 3×10^{10} Pa s.

6. Character of the Flow Pulses

[29] We observed only the very end of P0 and can say little about its development. P3 was also poorly sampled, but P1 and P2 are seen in their entirety. It is clear from the estimates that the extrusion rate did not remain constant and ranged between about 1.8 and 0.3 m^3 s^{-1} (Table 2), though the pulse-averaged extrusion rates for P1–3 fall in a much smaller range: 0.7–0.9 m^3 s^{-1}. The ends of pulses P1 and P2 were both characterized by low extrusion rates, and the highest rates occurred at the start of pulses P1 and P3. There is a tendency, therefore, for extrusion rate to fall during each pulse.

[30] Pulsatory behavior during the emplacement of lava flows has long been recognized qualitatively. Pulsation may occur on many lava flows, but it has been studied quantitatively in the channelized sections of flows where there is a clear local frame of reference against which to observe and measure the rise and fall of the flowing lava surface as the pulse passes downslope. Ground-based thermal imagery has been used as a proxy measurement of the volume flux of channelized lava flow on Etna during 2001, 2004 and 2008 [*Bailey et al.*, 2006; *James et al.*, 2007, 2010]. Pulses were observed to occur from a few minutes to about three hours apart. At the start of these wave-like pulses the speed of channel flow, the flow height and thermal signal all increased rapidly and then decayed much more slowly.

[31] *Favalli et al.* [2010] used multiple airborne lidar surveys of the 2006 lava flowfield of Etna to map pulses of lava more directly, using changing topography in channelized flow. They reported the steep front morphology of each pulse as observed with the thermal data and the rapid advance of flows rejuvenated by the arrival of a pulse in the distal zone. Pulses in the channel typically moved at maximum speeds of ~0.02–0.1 m/s in plug flow through cross sections of the order of 100 m^2, with lengths of the order of 200–100 m, to give fluxes in the range of 0.5–3 m^3 s^{-1} (Table 3).

[32] The pulsatory character of the andesitic Bagana flows shares some similarities with the basaltic flows at Etna: the steep front morphology, the tendency to spill over onto the levees as the front of the pulse passes and the rapid advance of the flow over new terrain when the pulse reached the distal zone. On Etna, up to 3–4 pulses of lava were observed to occupy the same channel [e.g., *Favalli et al.*, 2010] (Figure 7), while 2 pulses at most were observed simultaneously on Bagana. The overflows on Bagana tended to occur at the break of slope from about 25° to 15°, 1.5 km from the crater (Figure 2). But the main difference is that the scale of the pulses, mirroring the channel sizes, is much greater

Table 3. Approximate Ranges of Pulsed Flow Measurements at Etna and Bagana

Flow Characteristic Ranges	Etna [from *Favalli et al.*, 2010]	Bagana
Thickness (m)	3–10	20–90
Channel Width (m)	20–40	60–150
Flow advance (m/day)	250–1500	2–50
Extrusion rate (m^3 s^{-1})	0.5–3.5	0.3–1.8
Pulse length (m)	100–200	700–1200
Pulse volume (m^3)	3,000–20,000	6,000,000–17,000,000

on Bagana than Etna (Table 3). Although of comparable flux to Etna, the Bagana flows were much larger, slower moving and lasted much longer. However, we have not observed these flows at close quarters. It is not certain whether the Bagana pluses are thermomechanically continuous with the previous pulse, or are effectively separate flows that override the earlier flow, with a discontinuity between them.

[33] Figure 5 summarizes the ground-based and OMI-SO_2 observations with respect to the periods when the three pulses were initiated. At the start of P2 and P3, and to a lesser extent for P1, observations of incandescence increased, coupled with roaring, particularly during P3. Also SO_2 increased at the start of P1 and P3 and continued strongly over the following 1–2 months. These observations suggest that P2 probably began in late February 2011 and P3 began in late September 2011 (Figure 5). The other clear feature from the ground observations is that after initiation, P2 was characterized by explosions and ashfall with virtually no incandescence or roaring. Although these correlations are only qualitative, we interpret them as follows. The start of each pulse involved increased lava extrusion rate (incandescence) and gas flux (roaring from gas vent; increased atmospheric loading of SO_2). Later in P2 the lava and gas fluxes fell such that shallow gas pressure must have built before intermittent release (ash-bearing explosions).

7. Causes of Flow Pulsation

[34] The studies of flow pulses on Etna by *James et al.* [2007, 2010] concluded that while there were some observations of channel blockages and their subsequent failure initiating local surges in the channel, it was the variation in the magma flow rate prior to extrusion that was responsible for flow pulses, either through mass flux change or variable vesicularity. Observations of common fluctuations in multiple channels fed by separate vents also led *Favalli et al.* [2010] to consider that the pulses were generated within the vent-conduit, not as a result of surface processes.

[35] We now consider whether the pulsatory behavior of the Bagana lava flows might also have similar mechanisms, either within the feeding conduit or within the lava flow itself.

7.1. Bulk Rheological Change

[36] If the flux of lava supplied to any lava flow is constant, but the flow front decelerates or stops, then a new flow may begin upslope that makes its independent way down the drained or draining channel. We might expect the distal flow to thicken and broaden, maintaining the same flow rate. Cooling and crystallization of the flow or the

Figure 7. The mapped advance of the flow front positions on the dates shown, mainly for P2. The background change difference image is for 27 July–7 August 2011.

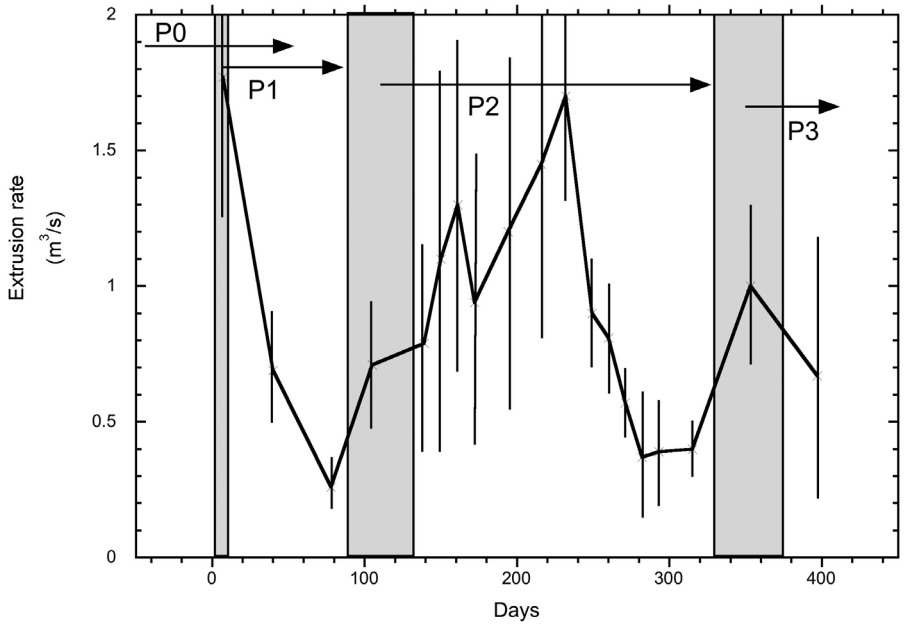

Figure 8. Extrusion rate variation with time (black line) estimated from each observation interval with the uncertainties represented as vertical lines in the middle of the intervals. The arrows indicate the four pulses (P0–P3) with the rectangles representing the uncertainty associated with the beginning of each pulse.

development of a crust might achieve this. *Kerr and Lyman* [2007] argued that the development of a crust with a strength of ~2 MPa in the distal part of the Lonquimay lava flow increased the bulk viscosity such that it eventually stopped the flow. However, the Lonquimay eruption is not reported to have involved separate pulses, and at Bagana P1 and P3 did not reach the same, 3 km, length that P0 and P2 did, which we might expect if time-dependent bulk rheological change was the control. Also, the estimates of lava flux at Bagana (Figure 8) show a far from constant pattern.

7.2. Supply Rate Variability

[37] If the supply rate of lava from the vent is variable in mass or volume then a sudden increase in that rate may initiate a new pulse. Also an explosion could disrupt the flow within the upper conduit sufficient to produce a hiatus in flow continuity and generate a new pulse. The observation of increased lava extrusion rate and gas flux at the 'initiation' of pulses on Bagana (Figure 8) suggests that the magma supply rate variation is the most likely explanation.

[38] But what might cause such variation? Heterogeneous gas contents in the conduit magma [e.g., *James et al.*, 2010] are unlikely for these much larger pulses. Variations in the rate of deep magma supply could be responsible for the pulsatory flow. A shallower mechanism to produce variability in magma flux was explored by *Costa et al.* [2007]. They showed that a multiweek cyclic variability in the growth of the Soufrière Hills Volcano, Montserrat lava dome could be modeled in terms of an elastic-walled dyke (between 1 and 5 km deep), storing and releasing magma. Such cycles were characterized by initial fluxes 2–3 times greater than those in the later stages. Figure 9 shows schematically for the P1–P2 period how such a shallow dyke storage mechanism might operate at Bagana. In Figure 9a the surface extrusion rate is low but the dyke is full of magma at high pressure fed from below at a continuous rate and would correspond to about day 80 of Figure 8. There must be some resistance to the upward flow from this dyke. This could be supplied by a conduit narrowing to choke flow, and/or nonlinear behavior of rheology of magma in the conduit [e.g., *Melnik and Sparks*, 1999]. This pressure begins to be relieved as a new pulse of lava is extruded at about day 120 of Figure 8 (Figure 9b) and the extrusion rate increases to a maximum at about day 220 (Figure 8) as the flow advances rapidly onto the lower slopes (Figure 9c). The volume of magma involved in these Bagana pulses is smaller (of the order of 10×10^6 m^3) and the cycle longer (up to 200 days) than the Soufrière Hills dyke-driven cyclicity

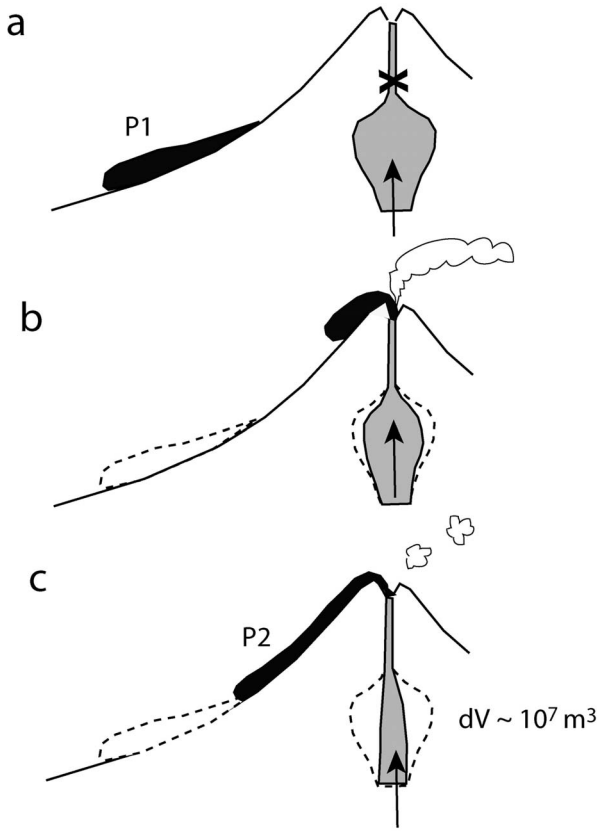

Figure 9. Shallow dyke storage model to explain pulsating lava flows. (a) A shallow, elastic-walled dyke receives magma at near constant rate from below, expands with an increase in magmatic pressure, but outflow to the surface is limited by a choke mechanism (cross). An earlier pulse of magma has emplaced lava flow P1. (b) Lava is extruded at a high rate, together with a high flux of sulphur dioxide. (c) Pressure, stored magma volume and surface extrusion rate fall as P2 lava advances over, or parallel to, P1 lava. Minor explosive gas release occurs.

(20–30 $\times$ 10^6 m^3 and 50 days respectively). The initial extrusion rates of the Soufrière Hills cycles were about 2–3 times the lowest rates, while at Bagana the factor is about 5.

8. Discussion and Conclusions

[39] High-frequency, high-spatial resolution spaceborne radar imaging is a powerful way to monitor the advance of the andesite lava flows of Bagana. The imaging characteristics of the TSX radar, particularly the 11-day revisit time, are well-suited to the relatively slow moving andesite lava flows, less so for basaltic flows that are emplaced much faster. In our study we have relied on relatively crude techniques to calculate flow volumes. The phase information from the TSX data could be used to estimate the surface topography of the 2010–11 lava using differential InSAR techniques. However, the radar response of the active parts of the lava flow becomes de-correlated over the 11 days required to form the interferometric pair. A potentially more satisfactory route to acquiring surface topography would be to use the single-pass interferometric technique available from the TanDEM-X satellites. This could give topographic information from even the most active flows, though there would be some line-of-sight limitations. However, data from this system are not yet available for Bagana.

[40] Our 21 radar images revealed the following:

[41] 1. From at least October 2010 to December 2011 continuous lava extrusion occurred on the western slopes of Bagana.

[42] 2. The blocky, andesite lava flow extended in two branches to 3 km, was 100–300 m wide, 20–90 m thick, with a channel 50–150 m wide.

[43] 3. Over 14 months, four distinct pulses of lava advanced through the channel with a typical volume of about 10^7 m^3.

[44] 4. The average extrusion rate was 0.92 $\pm$ 0.35 m^3 s^{-1}, and within the limits of the measurements there is a tendency for the highest rates ($\sim$1.8 m^3 s^{-1}) to occur in the first part of each pulse and the lowest rates ($\sim$ 0.3 m^3 s^{-1}) to occur in the latter part of each pulse.

[45] 5. The extrusion rate variability and observations of degassing behavior suggest that the pulses are driven by magma supply variability, perhaps due to shallow magma storage.

Acknowledgments

[46] GW thanks NERC NCEO for funding under grant NE/EO15093/1. The TerraSAR-X data were supplied by DLR under project GEO0879. We thank S. Tarquini and an anonymous reviewer for their help in improving the paper.

References

Bailey, J. E., A. J. L. Harris, J. Dehn, S. Calvari, and S. K. Rowland (2006), The changing morphology of an open channel lava flow on Mt Etna, *Bull. Volcanol.*, *68*, 497–515, doi:10.1007/s00445-005-0025-6.

Borgia, A., S. Linneman, D. Spencer, L. D. Morales, and J. B. Brenes (1983), Dynamics of lava flow fronts, Arenal Volcano, Costa Rica, *J. Volcanol. Geotherm. Res.*, *19*, 303–329, doi:10.1016/0377-0273(83)90116-6.

Breit, H., T. Fritz, U. Balss, M. Lachaise, A. Niedermeier, and M. Vonavka (2010), TerraSAR-X SAR processing and products, *IEEE Trans. Remote Sens*, *48*(2), 727–740, doi:10.1109/TGRS.2009.2035497.

Bultitude, R. J. (1976), Eruptive history of Bagana Volcano, Papua New Guinea, between 1882 and 1975, in *Volcanism in Australasia*, edited by R. W. Johnson, pp. 317–336, Elsevier, Amsterdam.

Bultitude, R. J. (1981), Note on activity from Bagana volcano from 1975 to 1980, in *Cooke-Ravian Volumes of Volcanological Papers*, edited by R. W. Johnson, *Geol. Surv. Papua New Guinea Mem.*, *10*, 243–248.

Bultitude, R. J., R. W. Johnson, and B. W. Chappell (1978), Andesites of Bagana Volcano, Papua New Guinea: Chemical stratigraphy, and a reference andesite composition, *BMR J. Aust. Geol. Geophys.*, *3*, 281–295.

Cigolini, C., A. Borgia, and L. Casertano (1984), Intra-crater activity, aa-block lava, viscosity and flow dynamics: Arenal Volcano, Costa Rica, *J. Volcanol. Geotherm. Res.*, *20*, 155–176, doi:10.1016/0377-0273(84)90072-6.

Costa, A., O. Melnik, R. S. J. Sparks, and B. Voight (2007), Control of magma flow in dykes on cyclic lava dome extrusion, *Geophys. Res. Lett.*, *34*, L02303, doi:10.1029/2006GL027466.

Favalli, M., A. Fornaci, F. Mazzarini, A. Harris, M. Neri, B. Behnke, M. T. Pareschi, S. Tarquini, and E. Boschi (2010), Evolution of an active lava flow field using a multitemporal LIDAR acquisition, *J. Geophys. Res.*, *115*, B11203, doi:10.1029/2010JB007463.

Gill, J. B. (1981), *Orogenic Andesites and Plate Tectonics*, 390 pp., Springer, New York, doi:10.1007/978-3-642-68012-0.

Griffiths, R. W. (2000), The dynamics of lava flows, *Annu. Rev. Fluid Mech.*, *32*, 477–518, doi:10.1146/annurev.fluid.32.1.477.

Harris, A. J. L., W. I. Rose, and L. P. Flynn (2003), Temporal trends in lava dome extrusion at Santiaguito 1922–2000, *Bull. Volcanol.*, *65*, 77–89.

Harris, A. J. L., L. P. Flynn, O. Matias, W. I. Rose, and J. Cornejo (2004), The evolution of an active silicic lava flow field: An ETM+ perspective, *J. Volcanol. Geotherm. Res.*, *135*, 147–168, doi:10.1016/j.jvolgeores.2003.12.011.

Harris, A. J. L., J. Dehn, and S. Calvari (2007), Lava effusion rate definition and measurement: A review, *Bull. Volcanol.*, *70*, 1–22, doi:10.1007/s00445-007-0120-y.

Hulme, G. (1974), The interpretation of lava flow morphology, *Geophys. J. R. Astron. Soc.*, *39*, 361–383, doi:10.1111/j.1365-246X.1974.tb05460.x.

James, M. R., H. Pinkerton, and S. Robson (2007), Image-based measurement of flux variation in distal regions of active lava flows, *Geochem. Geophys. Geosyst.*, *8*, Q03006, doi:10.1029/2006GC001448.

James, M. R., H. Pinkerton, and M. Ripepe (2010), Imaging short period variations in lava flux, *Bull. Volcanol.*, *72*, 671–676, doi:10.1007/s00445-010-0354-y.

Kerr, R. C., and A. W. Lyman (2007), Importance of surface crust strength during the flow of the 1988–1990 andesite lava of Lonquimay Volclano, Chile, *J. Geophys. Res.*, *112*, B03209, doi:10.1029/2006JB004522.

LaPrade, G. L., and E. S. Leonardo (1969), Elevations from radar imagery, *Photogramm. Eng.*, *29*(2), 366–371.

McCormick, B., M. Edmonds, T. Mather, and S. A. Carn (2012), First synoptic analysis of volcanic degassing in Papua New Guinea, *Geochem. Geophys. Geosyst. 13*, Q03008, doi:10.1029/2011GC003945.

McGonigle, A. J. S., C. Oppenheimer, V. I. Tsanev, S. Saunders, K. Mulina, S. Tohui, J. Bosco, J. Nahou, J. Kuduon, and F. Taranu (2004), Sulphur dioxide fluxes from Papua New Guinea's volcanoes, *Geophys. Res. Lett.*, *31*, L08606, doi:10.1029/2004GL019568.

Melnik, O., and R. S. J. Sparks (1999), Nonlinear dynamics of lava dome extrusion, *Nature*, *402*, 37–41, doi:10.1038/46950.

Naranjo, J. A., R. S. J. Sparks, M. V. Stasiuk, H. Moreno, and G. J. Ablay (1992), Morphological, structural and textural variations in the 1988–1990 andesite lava of Lonquimay Volcano, Chile, *Geol. Mag.*, *129*, 657–678, doi:10.1017/S0016756800008426.

Wadge, G., et al. (2008), Lava dome growth and mass wasting measured by a time series of ground-based radar and seismicity observations, *J. Geophys. Res.*, *113*, B08210, doi:10.1029/2007JB005466.

Wadge, G., P. Cole, A. Stinton, J.-C. Komorowski, R. Stewart, and A. C. Toombs (2011), Rapid topographic change measured by high resolution satellite radar at Soufriere Hills Volcano, Montserrat, 2008–2010, *J. Volcanol. Geotherm. Res.*, *199*, 142–152, doi:10.1016/j.jvolgeores.2010.10.011.